



Cellulose fiber-reinforced thermosetting composites: impact of cyanoethyl modification on mechanical, thermal and morphological properties

Md Rezaur Rahman¹ · Sinin Hamdan¹ · Zainab Binti Ngaini² ·
Elammaran Jayamani³ · Akshay Kakar¹ · Muhammad Khusairy Bin Bakri^{1,2} ·
Fahmi Asyadi Bin Md Yusof⁴

Received: 28 July 2018 / Revised: 4 October 2018 / Accepted: 2 November 2018 / Published online: 12 November 2018
© Springer-Verlag GmbH Germany, part of Springer Nature 2018

Abstract

This study explores the mechanical, thermal and morphological properties of untreated and cyanoethyl-treated *kempas* wood sawdust cellulose fiber-reinforced unsaturated polyester composites. The fiber loadings of the composites were varied from 0 to 20 wt%, with the increment of 5 wt%. The composites were tested for water absorption, and their FTIR spectroscopy, SEM and TGA results were analyzed. The FTIR results show that the fiber treatment reduces the hydroxyl groups in the cellulose, replacing them with the cyanoethyl groups. The TGA results show that the composites are stable up to 324 °C. SEM images of the treated fiber composites showed that there were no visible gaps between fibers and matrix which indicates a strong interfacial bond. From the mechanical tests, 15 wt% fiber loading composite was strongest. Among all the composites, cyanoethyl cellulose fiber unsaturated polyester composites had the most desirable mechanical and thermal properties, whereas the fiber treatment showed the improvement of interfacial bonding.

Abbreviations

CECFUPC	Cyanoethyl cellulose fiber unsaturated polyester composites
WF	Wood fiber
WS	Wood sawdust

✉ Md Rezaur Rahman
rmrezaur@unimas.my

- ¹ Faculty of Engineering, Universiti Malaysia Sarawak, Jalan Datuk Mohammad Musa, 94300 Kota Samarahan, Sarawak, Malaysia
- ² Faculty of Resources Science and Technology, Universiti Malaysia Sarawak, Jalan Datuk Mohammad Musa, 94300 Kota Samarahan, Sarawak, Malaysia
- ³ Faculty of Engineering, Computing and Science, Swinburne University of Technology Sarawak Campus, Jalan Simpang Tiga, 93350 Kuching, Sarawak, Malaysia
- ⁴ Polymer Technology Section, Universiti Kuala Lumpur Malaysia - Institute of Chemical and Bioengineering Technology, 78000 Alor Gajah, Melaka, Malaysia

WPF	Wood pulp fiber
UPC	Unsaturated polymer composites
UP	Unsaturated polyester
CF	Cellulose fiber
CECF	Cyanoethyl cellulose fibers
WFUPC	Wood fiber unsaturated polyester composites
CFUPC	Cellulose fiber unsaturated polyester composites
DWPF	Delignified wood pulp fiber
AWPF	Alkaline-treated wood pulp fiber
MEKP	Methyl ethyl ketone peroxide
WFUPC	Wood fiber unsaturated polyester composites

Introduction

Over the past few years, the use of natural plant fibers in polymer composites as reinforcement has been increasing, especially for producing cost-effective engineering materials [1–4]. The techniques for processing cellulose fibers from the existing waste materials containing natural fibers have been studied extensively, mainly to enhance its compatibility as fibrous fillers in polymer composites [2, 5]. Synthetic polymers are associated with high strength and low density. They can be easily casted into any shape or cured with hardening agents at much lower operating conditions than those required for metals and ceramics [3]. Among all types of natural fiber, wood fiber (WF) from processed wood sawdust (WS) has received keen attention since it is abundantly available in the wood processing industries worldwide, leading to environmental problems, if not managed properly [2]. The wide applications of these short lignocellulose fibers with full utilization of their naturally found properties are necessary [4, 6]. The presence of cellulosic fibers extracted from WF provides a potential demand to be used as precursors to make strong and lightweight polymer composite fillers, which enhance their chemical properties [7]. Wood pulp fibers (WPF) were processed to WF via thermomechanical processing and reduced its cellulose content using chemical treatments. These types of fibers are well suited for surface treatment using acrylonitrile. Cyanoethylation was conducted on wood pulp cellulose and was found to have higher degree of reaction than other fibers like cotton [8]. This was due to the lower degree of polymerization, since the WPF have shorter chain lengths of wood than those of cotton.

The tensile strength of the unsaturated polyester composites (UPC) is primarily affected by five main factors, namely tensile properties of the matrix and the fiber materials, fiber aspect ratio, fiber loading, fiber orientation and the interfacial bonding between the matrix and the fiber [5]. The fiber-reinforced composites theory of Weibull weakest-link statistical analysis stated that within the crucial region a material's strength is strongly influenced by its weakest point [9]. Thus, it is essential that the fiber-matrix bond is strong in order to support the composite and allow the fibers to share the applied stress [9]. It is known that any pull out of the raw fibers causes the crack to propagate further without any transfer of the load to the fiber. Therefore, chemical modifications are needed to be carried out to improve the bonding between

the fiber and the matrix. The main disadvantage of the cellulose fiber is its hydrophilic nature, which hinders its bonding compatibility with hydrophobic polymers. It also has a high moisture absorption when in contact with water or kept in humid conditions. Therefore, surface modification of the cellulose is required to make it more hydrophobic for stronger adhesion with the hydrophobic unsaturated polyester (UP) resin.

Surface modification techniques are used to increase hydrophobicity on the surface of cellulose fiber (CF). These include the derivatization of the functional groups in cellulose, usually by alkylation and silanation [10]. Anhydrides have also been used for CF surface modification to make it more compatible with hydrophobic polymers, which improve the overall composite's mechanical strength. Many studies have been conducted for the current surface treatment cellulose-derived fiber-reinforced polymer composites. However, the studies on chemically treated fibers that are compatible with thermoset polymer composites are few, due to its complexity in properties before and after curing. UP resins are slightly hydrophilic in nature, which is mainly caused by the presence of some hydroxyl and carboxyl groups present in its chemical structure. However, when cross-linked with styrene, the hydroxyl and carboxyl groups to the bulk mass ratio decrease rapidly until the curing process is complete. Thus, this requires surface treatment of CFs filler to be less hydrophilic, which enables it to be linked with UP resin and form tighter bonds for better mechanical properties and thermo-stability.

Acrylonitrile has been used in the chemical treatment of cellulose fibers' surface to form cyanoethyl cellulose fibers (CECF). Acrylonitrile contains double bond carbon groups ($-C=C-$) and could be grafted to the surface of cellulose to form cyanoethyl groups. Most of these groups are substituted with the hydroxyl groups that indirectly change the surface polarity of natural fibers, which enhanced the wettability (or surface adhesiveness) of the UP resins to the fibers [11]. The CF surface treatment increases the tensile properties and thermo-stability. This treatment is also known to reduce the water absorption in of CFs and also increase its resistance to fungal attacks [12]. Moreover, this CF has also been applied and studied in the reinforcement of UP resins and studied.

This research focuses on CF obtained from wood sawdust from a tropical hardwood species (*kempas*) to form wood cellulose pulp fiber. These fibers were treated with cyanoethylation, dried and added to UP resin as reinforcing fibers to fabricate cyanoethyl cellulose fiber-reinforced unsaturated polyester composites (CECFUPC). In addition to the properties of the chemical composition, tensile, thermal, morphological, and water absorption of CECFUPC were obtained from analytical tests. The investigated results of wood fiber unsaturated polyester composites (WFUPC) and CECFUPC of the same fiber loadings were compared.

Experimental

Materials

Kempas wood sawdust (WS) was collected from Sarawak Forest Research Institute. Hydrogen peroxide, acetic acid, titanium (IV) oxide, potassium hydroxide and

acrylonitrile (AN) were collected from Merck, Germany. All chemicals were analytical reagent grade.

Methods

Preparation of wood pulp (WP)

200 g of wood sawdust (WS) was soaked in distilled water for approximately 16 h. The WS was loaded into a mixer-grinder vessel with water up to 2/3 of the vessel's height. The WS was then ground in a mixer-grinder for 30 min. The wood pulp (WP) was later poured into a glass sample flask and placed into a heated sonicator bath for ultrasonication for 1 h at 80 °C. The WP was taken out, and excess water was removed by pouring it out. The WP was loaded into a wide-neck round-bottom reaction flask for delignification.

Delignification of WP

The wide-neck round-bottom reaction flask containing the WP was placed into a heating mantle placed in a fume chamber. 500 g of bleaching solution was prepared by adding 248.75 g of 30 wt% hydrogen peroxide, 248.75 g of acetic acid and 2.5 g of titanium (IV) oxide into the reaction flask. A flat flange lid with 5 socket joints was placed onto the flask and fastened tight with a stainless steel ring clip. All the holes on the lid were covered with pieces of aluminum foil. A digital thermometer was inserted into a hole with its probe closed with more aluminum foil. The samples are allowed to boil in the bleaching solution at 130 °C for 3 h in a fume chamber. The temperature was observed from the digital electronic thermometer and the time recorded after a stable temperature is reached. After 3 h, the heater was turned off and the flask was left to cool to approximately room temperature. The delignified wood pulp fiber (DWPF) was poured into filter funnels lined with filter paper and was washed with a drop of dilute potassium hydroxide (KOH) solution to neutralize the acidic solution followed by distilled water to approximately pH7. The DWPF was left to dry on filter paper to remove excess water.

Alkaline treatment of DWPF

900 mL of 6 wt% potassium hydroxide (KOH) solution was prepared by adding 54 g of pellets of KOH into 846 g of water in a flask. 60 g of DWPF was added into the flask. The flask was placed into a sonicator with water bath at 80 °C and left for 10 min. The sonication was turned on, and the sample is treated for 2 h. The alkaline-treated wood pulp fiber (AWPF) was poured into filter funnels lined with filter paper for filtering. The AWPF was rinsed with distilled water until approximately pH-7. The AWPF was left to dry on filter paper to remove excess water and is kept in a closed container saturated with water.

Thermomechanical fibrillation via wet grinding and deep freezing of AWPf

500 g of AWPf was loaded into a mixer grinder with approximately 2/3 filled with water and was ground in a mixer grinder at fine speed for 30 min. The finely ground AWPf slurry was poured into a thick-walled polyethylene sample bottle and placed into a freezer with temperature set at $-73\text{ }^{\circ}\text{C}$. The sample was allowed to freeze for 24 h. The samples were taken out of the deep freezer, placed into warm water bath at $60\text{ }^{\circ}\text{C}$ and was left until the ice was thawed. The sample was filtered to remove excess water. This sample, called cellulose fiber (CF), was kept in a sample bottle in a dark and cool place. The CFs were loaded loosely without pressing onto filter paper and put into a convection oven set at $80\text{ }^{\circ}\text{C}$ for 2 h for drying. The sample was ground in a mixer grinder until no large clumps can be observed. The finely ground sample was loaded into a sample bottle sealed with aluminum foil. The samples were weighed, and the mass was recorded. Half of the sample was dried in the convection oven at $80\text{ }^{\circ}\text{C}$ until the mass was constant.

Cyanoethylation of CF surface modification treatment using acrylonitrile

100 g of CECF was loaded into a beaker and added with 200 g of 3 wt% potassium hydroxide solution. The alkaline wet CECF was filtered until most of the alkaline was removed. The alkaline-impregnated CECF was placed into a beaker, and 10 g of acrylonitrile (AN) solution was added. The mixture was mixed thoroughly for 3 min. The beaker was covered with aluminum foil. Small holes were punctured into the aluminum foil cover using a syringe needle. The sample was placed into the sonicator with water bath that was preheated to $65\text{ }^{\circ}\text{C}$. When the sample reached isothermal, the sonication and de-gas function was turned on and the sample was treated for 1 h. After the treatment, the sample was taken out and left to cool until the fibers temperature return to room temperature. The treated pulp fiber was loaded onto filter funnels lined with filter paper and was rinsed with a dilute acetic acid solution followed by distilled water until approximately pH 7. The sample was filtered and then dried in the convection oven at $80\text{ }^{\circ}\text{C}$ for 2 h. The sample was ground in the mixer grinder until no large clumps were observed. The finely ground sample was loaded into a sample bottle, sealed with aluminum foil. Small holes were punctured into the aluminum foil cover using a syringe needle. The samples were weighed, and the mass was recorded. The sample was dried in the convection oven at $80\text{ }^{\circ}\text{C}$ until the mass was constant. Figure 1 shows the process flowchart.

Composites preparation

A 2 parts of cast iron dog bone sample mold that produces 4 dog bone-shaped samples for tensile test was placed onto a thin polyethylene sheet, which exceeded its size than the edges of the mold sample by at least 10 cm. Both pieces of the mold were coated thoroughly using silicone spray on both sides. 120 g of unsaturated polyester (UP) resin and 3 g of hardening agent of methyl ethyl ketone peroxide (MEKP) were poured into an open plastic bag to achieve 40:1 resin-to-hardener ratio. This mélange was mixed thoroughly for 3 min, and the homogenous mixture



Fig. 1 Process flowchart

was poured into the mold. The mold was then placed under pressure of 7 MPa for 6 h, to cure the samples.

Once cured, the samples were extracted using a rubber mallet. The samples were placed against a light source to ensure that no bubbles had formed during the fabrication process. Five such samples, ones without bubbles or defects, were sent for edge trimming using a rotating ceramic mill. This process was repeated for the fiber loading (with WF, CF and CECF, respectively) in the UP resin set at 5 wt%, 10 wt%, 15 wt% and 20 wt%. The amount of MEKP added was weighed according to the weight of the UP resin added. The process was repeated with the filler substituted by CF and CECF.

Testing

Fourier transform infrared spectroscopy (FTIR) The fiber, neat-UP and UPC samples were dried until there was no reduction in their weight. The samples were then loaded into FTIR spectrometer (Shimadzu IRAffinity⁻¹). The number of scans was set to be 20, and the wavelength range was 4000–400 cm⁻¹. The transmittance spectra of the samples were measured, recorded and plotted with the percentage of transmittance (%) against the wavelength (cm⁻¹). The spectrograms were then analyzed for the peaks corresponding to the organic compounds' chemical groups and compared with the databases to identify the materials from the chemical composition. The changes in peak intensity between the spectra were noted and compared to identify the changes in the chemical composition of the materials after the chemical treatment and composites. The tests were done according to ASTM E168-16 [13] and ASM E1252-98 [14]

Thermo-gravimetric analysis (TGA) Thermo-gravimetric analysis (TGA) was performed using the TGA unit (PerkinElmer, Pyris 1 TGA). It was used to measure the thermal stability of the fiber samples, unsaturated polyester (UP) and the fiber-reinforced UPC. 5–10 mg of each of the finely ground samples was loaded in the aluminum sample pan and sealed with a lid. The aluminum pan was then placed into the wire basket, followed by the hand-down wire. The temperature range was set from 30 to 600 °C, and the heating rate was set at 20 °C min⁻¹. The nitrogen gas atmosphere was controlled for the test throughout the process until the end of the test. Oxygen gas was then injected into the chamber to burn the remaining material. The TGA curves were analyzed and comparisons were made between the three categories of UPC and also between samples containing the same fiber but with different fiber loadings. The activation energy was obtained through Broido method [15]. A graph was plotted, and a curve was generated that best fit a straight line and the slope reflected the activation energy. The initial temperature, T_i , maximum temperature, T_m , final tempera-

ture, T_f , initial weight, W_{Ti} , maximum weight, W_{Tm} , and the final weight, W_{Tf} , were tabulated, as shown in Table 1. The tests were done according to ASTM E1868-10 [16] and ASTM E1131-08 [17].

Scanning electron microscopy (SEM) The surface of the tensile test samples was observed under the scanning electron microscope (Hitachi TM3000). The samples were mounted on the carbon tape, which were taped unto aluminum plates and coated with an ultrathin film of gold with a sputter coater. The images are taken at magnifications $300\times$ and $1000\times$ to observe the morphology of the broken surfaces of the samples. The images were analyzed and compared. The test was done according to ASTM E2015-04 [18].

Tensile test The tensile properties of the composites were tested using Shimadzu Universal Testing analytical unit at the crosshead speed of 5 mm/min. The thickness of the sample was 5 mm. An average value of 5 samples for each weight percentage was calculated. The test was done according to ASTM D638-14 [19].

Water absorption test The water absorption test was conducted according to ASTM D570-98 [20]. The samples were dried in a convection oven for a 2 days at $50\text{ }^\circ\text{C}$, and their weight was recorded. The samples were then immersed in distilled water in individually labeled bottles. The samples were taken out, dried by pressing with the industrial wiping paper and weighed at 24 h intervals until there were 3 consecutive values with no changes, using a digital laboratory scale with $d=0.001\text{ g}$. The water uptake and diffusion rate were calculated for each sample.

Table 1 Thermal characteristics of CECFUPC

Filler content (wt%)	T_i ($^\circ\text{C}$) ^a	T_m ($^\circ\text{C}$) ^b	T_f ($^\circ\text{C}$) ^c	W_{Ti} (%) ^d	W_{Tm} (%) ^e	W_{Tf} (%) ^f	Activation energy, E_a (kJ/K)
5	324.23	396.26	467.92	89.03	45.34	4.85	99.99
10	323.97	401.92	468.25	88.95	37.55	5.59	95.59
15	340.62	427.03	524.31	89.49	52.46	11.89	115.32
20	324.14	402.35	468.36	89.22	37.66	5.61	64.71

^aTemperature corresponding to the beginning of mass loss

^bTemperature corresponding to the maximum rate of mass loss

^cTemperature corresponding to the end of mass loss

^dMass loss at temperature corresponding to the beginning of mass loss

^eMass loss at temperature corresponding to the maximum rate of mass loss

^fMass loss at temperature corresponding to the end of mass loss

Results and discussion

Fourier transform infrared spectroscopy (FTIR)

The FTIR spectrum of WF, CF and CECF were measured, recorded and plotted on the graphs of transmittance (%) against wavelength (cm^{-1}), as shown in Fig. 2. CF spectra primarily consists of cellulose which contains hydroxyl ($-\text{OH}$) indicated by stretching at the wavelength of 3336.03 cm^{-1} and 2333.97 cm^{-1} and also $\text{C}-\text{OH}$ groups at 1031.96 cm^{-1} [14, 15]. However, when grafted with acrylonitrile, these peaks decreased as shown in CECF. The cyanoethyl cellulose contains nitrile or cyano ($-\text{C}\equiv\text{N}$) groups with stretching frequency at $2340\text{--}2250 \text{ cm}^{-1}$ [21–24]. The $-\text{OH}$ groups significantly decreased due to the introduction of UP into the CECF matrix. This proved that the UP was suitable in CECF matrix that improved the interfacial bonding as reflected in SEM images. The FTIR of neat cured UP and CECFUPC samples with 10 wt% and 20 wt% CECF fiber loading is shown in Fig. 3. It was detected that the $-\text{OH}$ groups were significantly decreased due to the addition of cured UP to the CECF.

Thermo-gravimetric analysis (TGA)

The TGA graphs of CECFUPCs with 5 wt%, 10 wt%, 15 wt% and 20 wt% fiber loading are shown in Fig. 4.

The CECFUPCs rapid decomposition occurred between 328.2 and $482.1 \text{ }^\circ\text{C}$ and the residual weight dropped from 90 to 8%, indicating that CECFUPCs were generally quite stable under $300 \text{ }^\circ\text{C}$. The CECFUPC filler content does not affect initial decomposition (T_i) temperature. As the fiber loading is increased, the

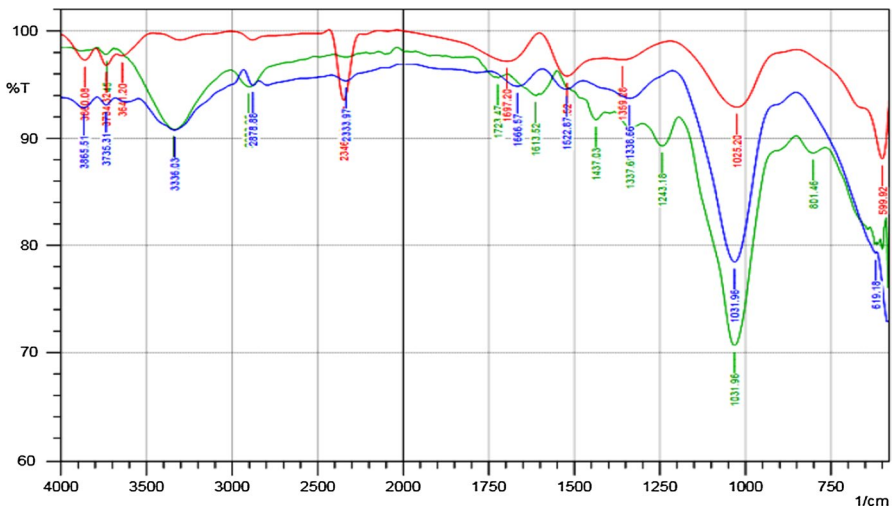


Fig. 2 FTIR spectrogram of (a) WF, (b) CF and (c) CECF

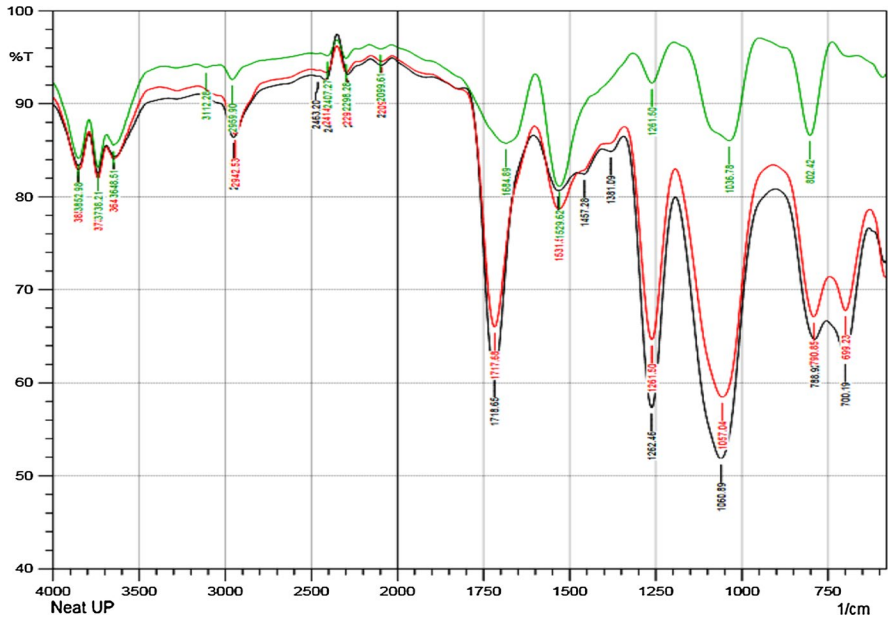


Fig. 3 FTIR spectrogram of (a) neat-UP, (b) 10 wt%CECFUPC and (c) 20 wt%CECFUPC

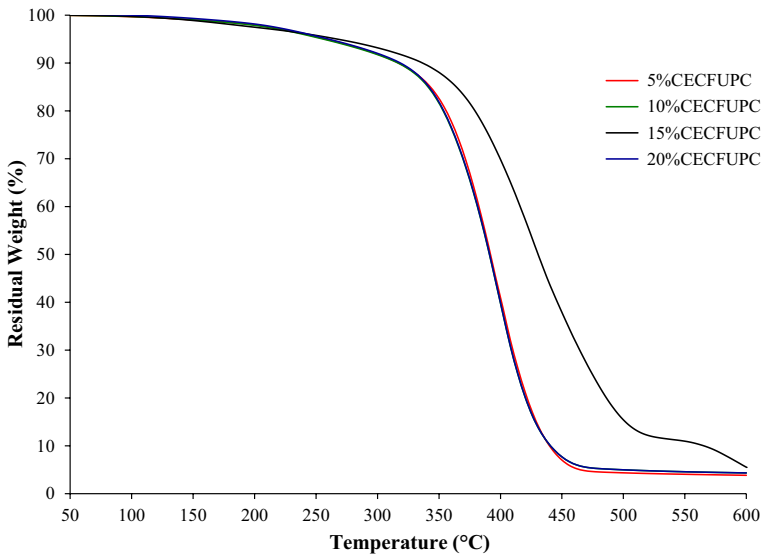


Fig. 4 TGA curves of 5 wt%CECFUPC, 10 wt%CECFUPC, 15 wt%CECFUPC and 20 wt%CECFUPC

temperatures at which the thermal decomposition started (T_f) gradually became higher. This indicates that higher CECF contents caused delayed thermal decomposition of CECFUPC. The W_{Ti} values showed that thermal decomposition started

was 85.37–90.52%, indicating that there were a high number of volatile components that had already broken and free from the composite, which formed carbon dioxide and other waste gases. The residual mass after the decomposition ended (W_{Tf}) of CECFUPCs was found to increase with an increase in the fiber loading. The most thermally stable composition was found to be 15 wt%CECFUPC. It had one of the highest residual mass at the starting point of thermal decomposition which starts at a relatively high temperature. 20 wt%CECFUPC also had a lower final decomposition temperature with one of the highest residual mass.

Below 300 °C, it was seen that the thermal stability of CECFUPCs were better than that of CFUPC's and WFUPC's. The WFUPC's had lower decomposition temperatures and also a lower residual mass after decomposition compared to CECFUPCs. The preliminary thermo-gravimetric study on the fibers showed that the rapid decomposition of CECF started at 266.4 °C, which was higher than the initial decomposition temperatures of CF (250.5 °C) and WF (260.6 °C). CECF also had a slower decomposition rate compared to WF and CECF. The initial decomposition residual weight of 94.74% for CECF at 95.08% is higher than CF (94.38%) and WF (93.95%). Therefore, CECF had the highest thermal stability among the fibers at temperatures due to the higher decomposition starting temperature compared to WF and a higher decomposition residual weight after decomposition than WF. This indicates that the chemical treatment performed on CECF, which substituted the hydrophilic groups on cellulose with cyanoethyl groups, had made the fibers more thermally stable. The cyanoethyl groups had improved the adhesive properties and created Van der Waal's forces between the cyanoethyl and unsaturated polyester groups.

The modified fibers had improved the thermal stability of the composites and the additional adhesive forces resulted in better thermal stability. The increase in thermal stability of fibers caused the CECFUPC to be more thermally stable compared to WFUPC and CFUPC. There was a higher amount of char produced from CF than CECF, caused by the carbon to non-carbon content ratio. The activation energy of the CECFUPCs showed that the higher the fiber content in the composite, the lower the activation energy required to initiate the decomposition reaction.

Scanning electron microscopy (SEM)

The SEM image of CECF of wood sawdust that was captured is shown in Fig. 5 at 1000× magnification. It was observed that the surfaces of the fibers were quite rough, making it more suitable for bonding with the matrix. The thickness and size of pores present in CECF were significantly reduced compared to WF, leaving some larger pieces of CECF with pores that were either elongated or compressed. These fibers indicated that the delignification reduced the fiber thickness and pore size by elimination of lignin and alkaline treatment removed hemicelluloses [25]. The fibers were weakened due to water absorption and desorption at its pores. After the fibers dried out, the structure became more rigid and maintained its initial shape. This increased the density and decreased weak regions that were found in the cellulose

Fig. 5 SEM image of CECF ($\times 1000$)

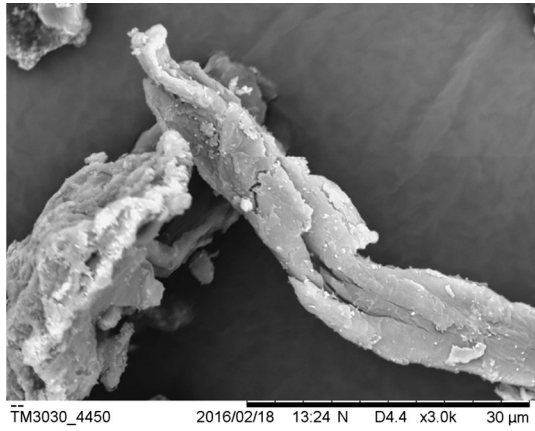


Fig. 6 SEM image of 5% CEC-FUPC at $\times 300$

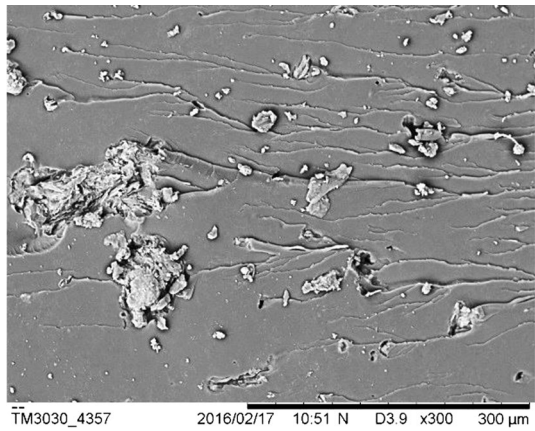


Fig. 7 SEM image of 10%CEC-FUPC at $\times 300$

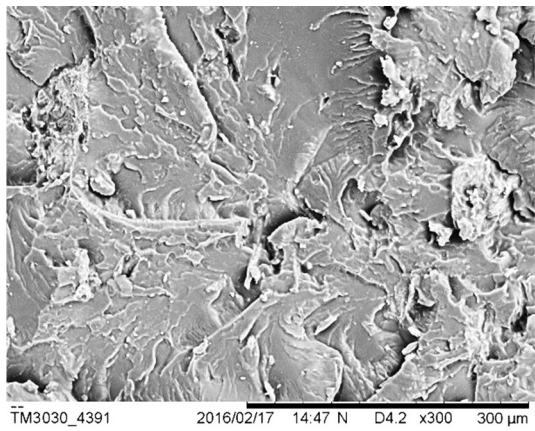


Fig. 8 SEM image of 15% CECFUPC at $\times 300$

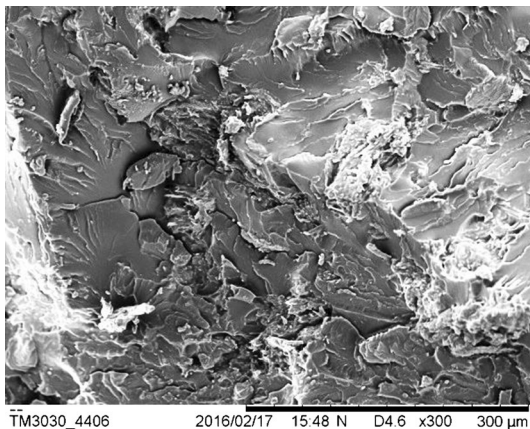
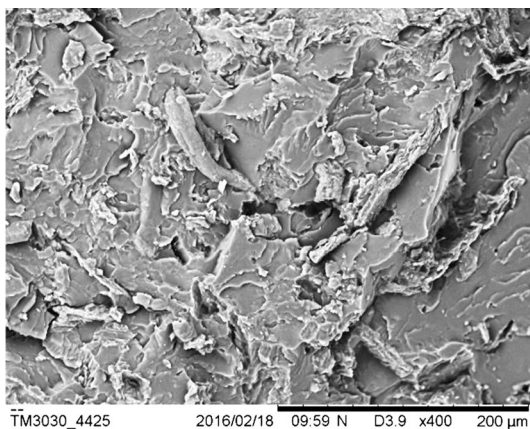


Fig. 9 SEM image of 20% CECFUPC at $\times 300$



fiber. The cyanoethylation process also contributed toward minimizing the pore size by coating the fiber surface and filling the voids partially.

The SEM images of the broken surface of CECFUPC tensile test samples with 5 wt%, 10 wt%, 15 wt% and 20 wt% CECF loading, as shown in Figs. 6, 7, 8 and 9, were taken at $300\times$ magnification. There are some long fibers as shown in Fig. 9 facing the fractured surface. There was random distribution of CECF in the composites with a slightly higher amount of fibers lying in an angle approximately parallel with the largest surface area of the CECFUPC tensile test sample. This showed that there was a high probability that the weakest points of the composite were within the region with the highest amount of fibers in the aforementioned direction.

The SEM images of the CECFUPC showed that the fractured surface of the composites had no visible spaces between fiber and matrix. This showed that the interfacial bond between the fiber surface and matrix was greatly improved, resulting in tensile strength and Young's Modulus higher than WFUPC and CFUPC [26]. The presence of deep cracks was also greatly reduced. The fracture started at the weakest point in the CECFUPC, propagating to the next weakest point, immediately next to

Table 2 Tensile properties of CECFUPC samples

Sample name	Tensile strength (MPa)	Young’s modulus (GPa)
5 wt%CECFUPC	28.93 (± 2.19)	1.39 (± 0.031)
10 wt%CECFUPC	29.93 (± 2.52)	1.57 (± 0.014)
15 wt%CECFUPC	31.59 (± 1.82)	1.91 (± 0.254)
20 wt%CECFUPC	28.47 (± 2.97)	1.71 (± 0.055)

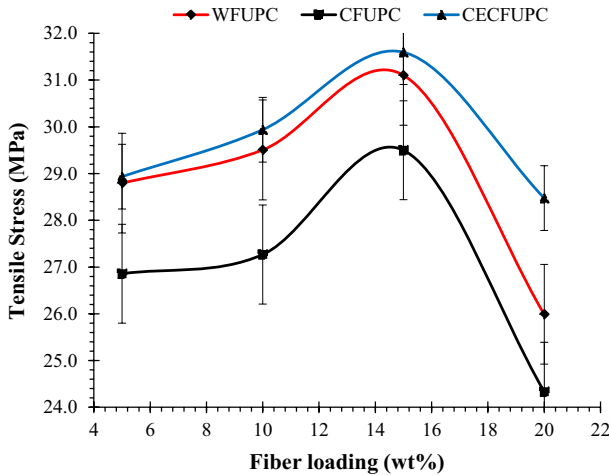


Fig. 10 Tensile strength of CECFUPC samples

it. The SEM images were compared with the tensile properties of CECFUPC. CECF had shared the load of the tensile forces and broke with the fiber tightly embedded with the larger body in the matrix with the end showing on the fractured surface.

Tensile properties

The mean tensile strength and Young’s modulus of CECFUPC samples are tabulated with their standard deviations in Table 2. 5 wt%CECFUPC had a tensile strength of 28.93 MPa (± 2.19 MPa) and a Young’s modulus of 1.39 GPa (± 0.035 GPa); 10 wt%CECFUPC had a tensile strength of 29.93 MPa (± 2.52 MPa) and a Young’s modulus of 1.57 GPa (± 0.014 GPa); 15 wt%CECFUPC had the highest tensile strength and Young’s modulus among the four types of CECFUPC, which was 31.59 MPa (± 1.82 MPa) and 1.91 GPa (± 0.25 GPa), respectively; 20 wt%CECFUPC had a tensile strength of 28.47 MPa (± 2.97 MPa) and a Young’s modulus of 1.51 GPa (± 0.055 GPa). Figure 10 shows the tensile strengths of the WFUPC’s, CFUPC’s and CECFUPCs. Figure 10 shows the values for the Young’s modulus of these three composites.

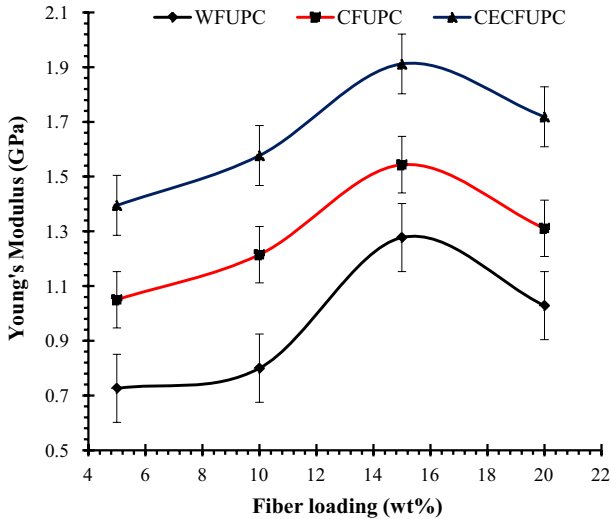


Fig. 11 Young's modulus of CECFUPC samples

Figures 10 and 11 show that the increase in CECF loading led to the increase in the tensile modulus. The Young's modulus increased with fiber loading of up to 15 wt% and then dropped at filler content of 20 wt%. This trend shows that the increase in fiber loading causes the composite tensile properties up to a certain point before it is overcome by limiting factors. The lower tensile strength 20 wt%CECFUPC is mainly due to lack of matrix to spread throughout the fibers, making the mixing rather difficult. The cured UP requires sufficient thickness to support the composite, and failing to achieve the minimum thickness will result in failure to support the tension and breaking. Another factor is the viscosity. The high fiber loading increases the viscosity of the filler-resin mixture. Therefore, it causes difficulty in mixing the two components of the composite and hinders the distribution of fiber in the composite. Since the tensile strength of the composite banks on the stress distribution within the composite, it is crucial for the fibers to be homogeneously distributed within the matrix.

Observing from Figs. 10 and 11, the comparison between same fiber loadings, respectively, showed that all the CECFUPCs had higher tensile strengths and Young's modulus values compared to the WFUPC's and CFUPC's. CECF are CF that were treated with acrylonitrile and grafted with cyanoethyl groups. This factor led to an increase in the tensile strengths. The FTIR graph indicated that the fibers' surface had been substituted with the cyanoethyl groups instead of hydroxyl groups. This indicates that the fibers had become more compatible with the UP matrix as it is influenced by the surface properties such as wettability with UP resin. The 10 wt%, 15 wt% and 20 wt%CECFUPC had higher Young's modulus values than that of cured neat-UP (1.47 GPa). The fibers showed the capability to enhance the elasticity of the UPC. Overall, the results showed less favorable reinforcement in tensile strength when UP was infused with CECF as filler. However, CECF had

greatly improved the elasticity of the UPC as indicated by the Young's Modulus. It was therefore concluded that the best fiber loading is 15 wt%CECFUPC because of the capability to reinforce the composite by enhancing its elasticity.

Water absorption

The results of water absorption test for the CECFUPC are shown in Fig. 12. The saturation points of the 5 wt%, 10 wt%, 15 wt% and 20 wt%CECFUPCs were 1.65%, 1.52%, 2.26% and 2.45%, respectively. The water absorbed by CECFUPC samples was twice as much as the amount absorbed by neat-UP (0.95%). The graphs showed that the water absorption rates were increased with the CECF loaded in the CECFUPCs. All of the CECFUPCs reached their saturation point after 19 days. The lines representing 5 wt%, 15 wt%, and 20 wt%CECFUPC fiber loadings had a clear layered pattern with almost no overlapping between lines except at the beginning.

When compared with water absorption results of WFUPC and CFUPC with the same fiber loading, it was found that the CECFUPCs had a slightly lower water absorbance compared to CFUPCs, except for the 5 wt%. This was due to the surface grafting of acrylonitrile to the surface to substitute the hydroxyl groups with cyanoethyl, causing the water absorbance of the fiber to be lowered. Moreover, they also had a lower water absorbance compared to the WFUPC samples except for the 15 wt% WFUPC. This showed that the treatment had successfully reduced the water absorption due to the reduction in fiber thickness and the replacement of hydroxyl groups of cellulose with the hydrophobic cyanoethyl groups. The SEM images showed that the CECF were tightly bonded with the UP matrix, indicating there are no big gaps for water to enter, implying that the CECFUPC only can absorb water from the surface. The chemical treatment using acrylonitrile on CF to form CECF

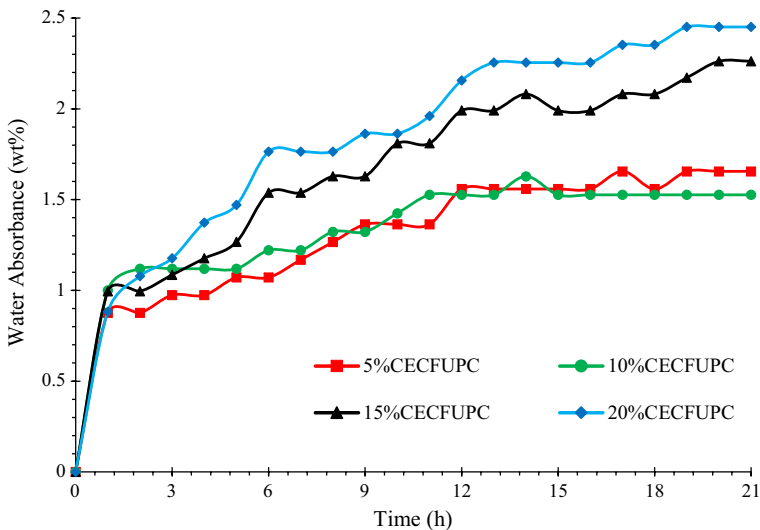


Fig. 12 Water absorption of CECFUPC in 21 days

had caused the fibers to be wrapped tightly by the cured UP matrix and reduced the probability of water entering the composite. The resistance of water absorbed by the fibers was found to decrease with the increase in fiber loading. Therefore, the best choice among the CECFUPC is 5 wt%CECFUPC. Similar results were obtained by Das and Biswas [27], Munoz and Garcia-Manrique [28] and Thakur and Singha [29].

Conclusions

In this research, the FTIR results showed that the treatment of CECF had lowered the hydroxyl groups in cellulose and replaced them with cyanoethyl groups from the wood pulp fibers. The 15 wt%CECFUPC had the highest tensile strength (31.6 MPa) and highest Young's Modulus (1.91 GPa) among all CECFUPC. The tensile properties of the CECFUPC were higher than WFUPC and CFUPC due to the compatibility between the CECF and UP matrix resulting in stronger interfacial bonds. The TGA results showed the CECFUPCs were quite thermally stable up to around 324 °C. The most thermally stable fiber loading for CECFUPC was 15 wt% because it had one of the highest residual mass at the starting point of thermal decomposition which starts at a relatively high temperature. The SEM image of the fibers showed that the fibers had been reduced in thickness and had a rougher surface and smaller pores due to the removal of the components surrounding CF and coated with cyanoethyl groups. SEM images of CECFUPC showed that there were no visible gaps between fibers. Due to the strong interfacial bond, the tensile strength and Young's modulus of CECFUPC are higher than WFUPC and CFUPC. The CECFUPC had most of the saturation points lower than that of WFUPC due to thinner fibers resulting in closer packing and better surface interfacial bonds. Overall, addition of CECF to UP matrix had produced UPC's with higher tensile strengths and Young's Modulus, increased thermo-stability and lowered water absorption compared to WFUPC and CFUPC.

Acknowledgements The authors are grateful for the support of Universiti Malaysia Sarawak (UNIMAS).

References

1. Jiang D, Xing L, Liu L, Yan X, Guo J, Zhang X, Zhang Q, Wu Z, Zhao F, Huang Y, Wei S, Guo Z (2014) Interfacially reinforced unsaturated polyester composites by chemically grafting different functional POSS onto carbon fibers. *J Mater Chem A* 43:18293–18303. <https://doi.org/10.1039/C4TA04055D>
2. Horta JF, Simões FJ, Mateus A (2017) Study of wood-plastic composites with reused high density polyethylene and wood sawdust. *Procedia Manuf* 12:221–229. <https://doi.org/10.1016/j.promfg.2017.08.026>
3. Gupta MC, Gupta AP (2005) Polymer composite. New Age International (P) Ltd, Delhi
4. Gallos A, Paës G, Allais F, Beaugrand J (2017) Lignocellulosic fibers: a critical review of the extrusion process for enhancement of the properties of natural fiber composites. *RSC Adv* 55:34638–34654. <https://doi.org/10.1039/C7RA05240E>

5. Jawaid M, Tahir PM, Saba N (2017) Lignocellulosic fibre and biomass-based composite materials. Woodhead Publishing Limited, Sawston
6. Bendahou A, Kaddami H, Sautereau H, Raihane M, Erchiqui F, Dufresne A (2008) Short palm tree fibers polyolefin composites: effect of filler content and coupling agent on physical properties. *Macromol Mater Eng* 293:140–148. <https://doi.org/10.1002/mame.200700315>
7. Dhakal HN, Zhang ZY, Richardson MOW (2007) Effect of water absorption on the mechanical properties of hemp fibre reinforced unsaturated polyester composites. *Compos Sci Technol* 67:1674–1683. <https://doi.org/10.1016/j.compscitech.2006.06.019>
8. Sefain MZ, Fadl MH, Elwakil NA, Naoum MM (1993) Kinetics of heterogeneous cyanoethylation of cellulose. *Polym Int* 32:251–255. <https://doi.org/10.1002/pi.4990320307>
9. Maalej M (2001) Tensile properties of short fiber composites with fiber strength distribution. *J Mater Sci* 36:2203–2212. <https://doi.org/10.1023/A:1017500218309>
10. Hubbe MA, Rojas OJ, Lucia LA, Sain M, Forest TA (2008) Cellulosic nanocomposites: a review. *BioResources* 3:929–980. <https://doi.org/10.15376/biores.3.3.929-980>
11. Li K, Qiu R, Liu W (2015) Improvement of interfacial adhesion in natural plant fiber-reinforced unsaturated polyester composites: a critical review. *Rev Adhes Adhes* 3:98–120. <https://doi.org/10.7569/RAA.2015.097301>
12. Shanks RA (2013) Cellulose-based nanocomposites: processing techniques. In: Dufresne A, Thomas S, Pothen LA (eds) *Biopolymer nanocomposites: processing, properties and applications*. Wiley, New York, pp 391–410
13. ASTM E168-16 (2016) ASTM Int, pp 1–18. <https://doi.org/10.1520/E0168-16>
14. ASTM E1252-98 (2013) ASTM Int, pp 1–13. <https://doi.org/10.1520/E1252-98R13E01>
15. Rana AK, Mandal A, Bandyopadhyay S (2003) Short jute fiber reinforced polypropylene composites: effect of compatibiliser, impact modifier and fiber loading. *Compos Sci Technol* 63:801–806. [https://doi.org/10.1016/S0266-3538\(02\)00267-1](https://doi.org/10.1016/S0266-3538(02)00267-1)
16. ASTM E1868-10 (2015) ASTM Int, pp 1–6. <https://doi.org/10.1520/E1868-10R15>
17. ASTM E1131-08 (2014) ASTM Int, pp 1–6. <https://doi.org/10.1520/E1131-08R14>
18. ASTM E2015-04 (2014) ASTM Int, pp 1–10. <https://doi.org/10.1520/E2015-04R14>
19. ASTM D638-14 (2014) ASTM Int, pp 1–17. <https://doi.org/10.1520/D0638-14>
20. ASTM D570-98 (2010) ASTM Int, pp 1–4. <https://doi.org/10.1520/D0570-98R10E01>
21. Bodirlau R, Teaca CA (2009) Fourier transform infrared spectroscopy and thermal analysis of lignocellulose fillers treated with organic anhydrides. *Rom J Phys* 54:93–104
22. González-Peña MM, Hale MDC (2011) Rapid assessment of physical properties and chemical composition of thermally modified wood by mid-infrared spectroscopy. *Wood Sci Technol* 45:83–102. <https://doi.org/10.1007/s00226-010-0307-9>
23. Titcombe LA (1994) Chemically modified cotton linters: preparations and papermaking properties. Ph.D. Thesis, University of Tasmania. <https://eprints.utas.edu.au/17700/>. Accessed 23 Mar 2018
24. Kamel S, Hassan EM, El-Sakhawy M (2006) Preparation and application of acrylonitrile-grafted cyanoethyl cellulose for the removal of copper (II) ions. *J Appl Polym Sci* 100:329–334. <https://doi.org/10.1002/app.23317>
25. Jia S, Fei J, Zhou J, Chen X, Meng J (2009) Direct electrochemistry of hemoglobin entrapped in cyanoethyl cellulose film and its electrocatalysis to nitric oxide. *Biosens Bioelectron* 24:3049–3054. <https://doi.org/10.1016/j.bios.2009.03.022>
26. Rahman MR, Ting JSH, Hamdan S, Hasan M, Salleh SF, Rahman MM (2016) Impact of delignification on mechanical, morphological, and thermal properties of wood sawdust reinforced unsaturated polyester composites. *J Vinyl Addit Technol* 24:185–191. <https://doi.org/10.1002/vnl.21545>
27. Das G, Biswas S (2016) Physical, mechanical and water absorption behaviour of coir fiber reinforced epoxy composites filled with Al₂O₃ particulates. *IOP Conf Ser Mater Sci Eng* 115:012012. <https://doi.org/10.1088/1757-899X/115/1/012012>
28. Munoz E, Garcia-Manrique JA (2015) Water absorption behaviour and its effect on the mechanical properties of flax fibre reinforced bioepoxy composites. *Int J Polym Sci* 2015:1–10. <https://doi.org/10.1155/2015/390275>
29. Thakur VK, Singha AS (2010) Mechanical and water absorption properties of natural fibers/polymer biocomposites. *Polym Plast Technol Eng* 49:694–700. <https://doi.org/10.1080/03602551003682067>